













Article

Machine Learning Methods for Predicting Cancer Complications Using Smartphone Sensor Data: A Prospective Study

Gabrielė Dargė¹ , Gabrielė Kasputytė¹ , Paulius Savickas¹, Adomas Bunevičius² , Inesa Bunevičienė³ , Erika Korobeinikova⁴ , Domas Vaitiekus⁴ , Arturas Inčiūra⁴ , Laimonas Jaruševičius⁴ , Romas Bunevičius⁵ , Ričardas Krikštolaitis¹ , Tomas Krilavičius^{1,*}  and Elona Juozaitytė⁴ 

- ¹ Faculty of Informatics, Vytautas Magnus University, Studentų 10, Kaunas District, LT-53361 Akademija, Lithuania; gabriele.darge@vdu.lt (G.D.); gabriele.kasputyte@vdu.lt (G.K.); paulius.savickas@vdu.lt (P.S.); ricardas.krikstolaitis@vdu.lt (R.K.)
- ² Vagelos College of Physicians and Surgeons, Columbia University, New York, NY 10033, USA; a.bunevicius@yahoo.com
- ³ Faculty of Political Science and Diplomacy, Vytautas Magnus University, LT-44212 Kaunas, Lithuania; inesa.buneviciene@vdu.lt
- ⁴ Oncology Institute, Lithuanian University of Health Sciences, LT-45434 Kaunas, Lithuania; erikakorobeinikova@gmail.com (E.K.); domas.vaitiekus@kaunoklinikos.lt (D.V.); arturas.inciura1@gmail.com (A.I.); laimonas.jarusevicius@kaunoklinikos.lt (L.J.); elona.juozaityte@kaunoklinikos.lt (E.J.)
- ⁵ ProIT, LT-09312 Vilnius, Lithuania; romas.bunevicius@proit.lt
- * Correspondence: tomas.krilavicius@vdu.lt

Abstract

Complications are frequent in cancer patients and contribute to adverse outcomes and higher healthcare costs, underscoring the need for earlier identification and prediction. This study evaluated the feasibility of using passively generated smartphone sensor data to explore early-warning signals of complications and symptom worsening during cancer treatment. A total of 108 patients were continuously monitored using accelerometer, GPS, and screen on/off data collected through the LAIMA application, while symptoms of depression, fatigue, and nausea were assessed every two weeks and complications were confirmed during clinic visits or emergency presentations. Smartphone data streams were aggregated into variables describing activity and sociability patterns. Machine learning models, including Decision Tree, Extreme Gradient Boosting, K-Nearest Neighbors, and Support Vector Machine, were used for complication prediction, and time-series models such as Autoregressive Integrated Moving Average, Holt–Winters, TBATS, Long Short-Term Memory neural network, and General Regression Neural Network were applied to identify early behavioral changes preceding symptom reports. In this exploratory analysis, the ensemble model demonstrated high sensitivity (89%) for identifying complication events. Smartphone-derived behavioral indicators enabled earlier detection of depression, fatigue, and vomiting by about nine days in a subset of patients. These findings demonstrate the feasibility of passive smartphone sensor data as exploratory early-warning signals, warranting validation in larger cohorts.

Keywords: cancer complications; smartphone sensors; digital phenotyping; machine learning



Academic Editors: Gang Wei and Gemma Leone

Received: 19 November 2025

Revised: 20 December 2025

Accepted: 23 December 2025

Published: 25 December 2025

Copyright: © 2025 by the authors.

Licensee MDPI, Basel, Switzerland.

This article is an open access article distributed under the terms and conditions of the [Creative Commons Attribution \(CC BY\) license](https://creativecommons.org/licenses/by/4.0/).

1. Introduction

In 2020, cancer accounted for nearly 10 million deaths globally, comprising one out of every six fatalities [1]. Cancer patients are at high risk for physical and psychological challenges resulting from either cancer or adverse effects of cancer treatments [2–5].

Surgery, chemotherapy, and radiotherapy—the cornerstone treatments in oncology—are frequently associated with serious complications [6–8], which may require ED visits or hospital admissions, impair quality of life, limit treatment options and generate substantial healthcare costs [9].

Remote monitoring is emerging as an important tool for comprehensive oncology care [10,11]. Increasing utilization of remote patient monitoring [12–15] is expected to improve detection of complications and symptoms, leading to improved healthcare outcomes and quality of life for individuals with chronic conditions or undergoing postoperative care [16]. Smartphones are an attractive method for remote monitoring in healthcare due to embedded sensors allowing real-time monitoring of individuals' behavior at low cost [17].

Prior studies used machine learning methods to analyze smartphone sensor data to predict depression, anxiety, and sleep disturbance [18], anastomotic leakage and pulmonary complications [19], frailty, mortality, and complications associated with metastatic spine tumor surgery [20], and cluster symptoms in patients with cancer [21–25], demonstrating promising results. While electronic patient-reported outcome (PRO) systems such as eRAPID have demonstrated clinical benefits during cancer treatment, they rely on active patient reporting and capture symptom burden after deterioration becomes apparent [26]. Systematic reviews of digital phenotyping show that passively collected smartphone data can reflect clinically meaningful behavioral changes, but most studies focus on mental health populations, single-sensor data, or population-level associations, with limited application in oncology [27]. In contrast, the present study leverages multi-sensor passive smartphone data (accelerometer, GPS, and screen-state) to model individualized behavioral baselines during active cancer treatment. By integrating machine learning–based short-term complication prediction with personalized time-series deviation detection, our approach aims to provide an early-warning signal preceding clinical presentation or self-reported symptom worsening, complementing rather than replacing PRO-based monitoring.

Several studies have applied artificial intelligence (AI) methods to predict or classify treatment-related complications across different clinical contexts. A commonly used approach in previous work is Support Vector Machines (SVM). One study [28] used SVM and gradient boosting (XgBoost) to predict complications after pancreatoduodenectomy, while another [29] used SVM to predict postoperative complications after anterior cervical discectomy and fusion. Other studies applied Neural Networks, Naïve Bayes, Decision Tree, SVM, Random Forest and Bayesian Network models to predict esophageal varices [30] gastrointestinal leaks and venous thromboembolism [31], and complications of advanced schistosomiasis [32].

Time-series approaches are also widely used in medical prediction tasks. For example, ARIMA was applied to forecast symptom complexity in an oncology clinic [33], Holt–Winters to model infectious-disease clinic visits [34], LSTM networks to predict dengue incidence [35], and GRNN/PNN models to predict oral cancer [36].

Prior studies have applied machine learning to smartphone sensor data to predict mental health symptoms, postoperative complications, or disease-related behaviors; however, none have combined accelerometer, GPS, and screen-state data during active cancer treatment to identify general complications or early symptom deterioration. In this study, we introduce a unified methodological framework that transforms continuously collected multi-sensor smartphone data into individualized behavioral deviation signals, enabling short-term prediction of cancer-related complications and early detection of symptom deterioration during active treatment.

This study aimed to develop and explore the feasibility of a multi-stage analytical framework that integrates passively generated smartphone sensor data with machine learning and time-series modeling to (i) predict imminent cancer-related complications and

(ii) detect early behavioral deviations preceding self-reported symptom worsening during active cancer treatment.

The primary contribution of this study is the demonstration of the feasibility of an integrated, multi-sensor, patient-specific analytical framework for exploratory early-warning signal detection during active cancer treatment. Specifically, we show how passively collected accelerometer, GPS, and screen-state data can be transformed into individualized behavioral baselines and short-term deviation signals. Performance metrics and early-detection results are presented as illustrative and hypothesis-generating, rather than confirmatory or generalizable.

2. Methods

2.1. Study Population and Procedures

This prospective observational study included patients undergoing treatment for cancer at the Hospital of Lithuanian University of Health Sciences Kaunas Clinics in Kaunas, Lithuania. The study inclusion criteria were: (1) cancer diagnosis; (2) current active treatment or surveillance for cancer; (3) ability to understand Lithuanian; (4) ownership of a smartphone; (5) age of 18 years or older; and (6) ability to provide informed consent. There were no exclusion criteria regarding cancer diagnosis or type of active treatment. The study period was from August 2022 until September 2023.

The study protocol and its consent procedure were approved by the Bioethics Committee, Kaunas, Lithuania. All participants gave signed informed consent before inclusion in the study.

At the initial study visit, investigators recorded baseline demographic and clinical information and registered eligible patients in the study portal (<https://laima2-2.proit.lt/>) accessed on 12 December 2025. The LAIMA application was installed on participants' personal smartphones, and participants were provided with credentials and instructions regarding voluntary withdrawal procedures. Passively generated data were collected continuously throughout the study period, while actively collected data included the European Organization for Research and Treatment of Cancer Core Quality of Life questionnaire (EORTC QLQ-C30), administered every two weeks [37]. To improve reproducibility and methodological clarity, additional monitoring procedures were implemented, including automated checks for data-flow interruptions and daily completeness indicators stored in log files.

2.2. Demographic and Clinical Information

Demographic information included age, sex, education, marital status, and occupation. Clinical information included cancer diagnosis, current and previous treatments (systemic treatment and radiotherapy), and Eastern Cooperative Oncology Group (ECOG) performance status. Board-certified oncologists on the LAIMA platform recorded all clinical and demographic data. Cancer diagnosis and treatment history were extracted from electronic medical records, while ECOG status was assigned at the baseline clinical visit. No stratification by cancer type or treatment modality was performed due to the small sample size.

2.3. Passively Generated Data

This study used the LAIMA application to collect passively generated data from personal smartphone sensors. The LAIMA application was developed based on the open-source Beiwe platform (<https://eu.beiwe.org/>, accessed on 12 December 2025) and is supported by iOS and Android operating systems. In addition to data collection, the platform enables secure patient registration and remote monitoring through an integrated

web interface. The LAIMA platform and application comply with the requirements of the General Data Protection Regulation (GDPR) of the European Union [38]. A normalization procedure was applied to minimize variability introduced by differences in smartphone hardware and operating systems, ensuring comparability of sensor-derived measures across devices. To protect privacy, raw GPS coordinates were never stored; instead, only derived mobility features (distance, time at home, POI counts) were saved.

Overall, 108 patients were included in this study with different follow-up time (Figure 1).

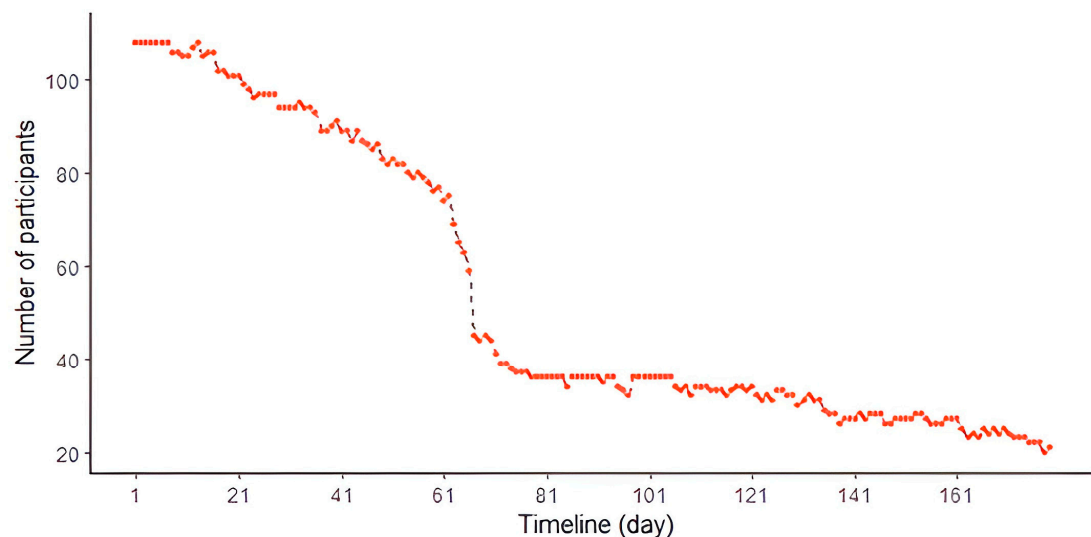


Figure 1. Passively generated data—during trial.

Several types of data, including accelerometer, GPS, log files, and power state data, were collected, analyzed, and aggregated. An accelerometer’s data consists of: (1) timestamp; (2) x coordinates; (3) y coordinates; (4) z coordinates. Raw accelerometer values were aggregated to 1 s resolution and normalized using formula:

$$x_{norm} = x / \max |x|, \quad (1)$$

where x_{norm} —normalized value, x —real value, and $\max |x|$ —the maximum of absolute value.

The following variables were determined using accelerometer data: duration of activity, duration of exertional activity and duration of active period.

To improve reproducibility, we explicitly describe the preprocessing steps: (1) per-minute variance of x, y, z axes was computed; (2) minutes with variance $< 0.0001 \text{ g}^2$ were classified as “no-movement” periods; (3) minutes with variance $> 0.15 \text{ g}^2$ were labeled as strenuous activity; (4) steady-state periods were merged using movement period length (MPL) equal to 60 min and movement pause period (MPP) equal to 2 min.

GPS data consist of timestamp, longitude, latitude, and altitude. Coordinated were aggregated to 1 s intervals and processed using the pointDistance function to calculate geodetic displacement between consecutive points [39]. The following variables were determined using GPS data: the duration of movement, the average speed, the average walking speed, the time spent in the most frequently visited place (home), the average distance to that place, and the number of places of interest (POI) per day. We specify that home was determined by modal coordinates recorded between 02:00–05:00 (given that the patient is not receiving inpatient treatment), assigning a radius of 10 m as the home region.

The power state data consists of the following: (1) timestamp; (2) event (Screen on/off). Screen on were computed by subtracting consecutive timestamp pairs and summing intervals within each day.

Daily log files were used to assess data-flow integrity by counting “Create new data files” events. The durations of the collected data were normalized and the ratio calculated based on this additional log information, protecting against data-flow issues.

The variables created from passively generated data are described in Table 1.

Table 1. Variables of passive data.

Variable	Sensor Used to Create the Variable	Description
Activity duration ratio	Accelerometer	The ratio of physical activity duration per day. The calculation follows these steps: (1) The variance of accelerometer coordinates is being calculated for each minute: $v(d, m) = v_x(d, m) + v_y(d, m) + v_z(d, m)$, where v_x —the variance of x coordinate values, v_y —the variance of y coordinate values, v_z —the variance of z coordinate values, d —day, and m —minute. (2) Periods of unchanging phone status are identified: if the variance of coordinates is less than a threshold of 0.0001 g^2 , it is assumed that the phone state does not change for that minute [40]. (3) All periods of steady phone states are summed up.
Exertional activity duration ratio	Accelerometer	The ratio of exertional physical activity duration per day. If the variance of coordinates is more than a threshold of 0.15 g^2 , it is assumed the phone state is changing for that minute and the exertional activity is identified [40]. All those minutes per day are summed up.
Active period	Accelerometer	Active period per day. To identify active period, firstly, the passive period is identified. The nearest periods of unchanged states are combined: since the patient can be active during the passive period, the adjacent periods of the unchanged states are combined, which are not less than the minimum permissible length of the period of the unchanged state and between which the active period does not exceed the maximum permissible period of activity. After testing, the optimal MPL is set to 60 min and the MPP is 2 min. The rest period of the day is denoted to active period.
Speed	GPS	The average speed per day (km/h).
Walking/jogging speed	GPS	The average speed (km/h) for movement classified as walking/jogging (<10 km/h).
Movement duration ratio	GPS	The ratio of movement duration per day (walking/jogging).
Time spent at home ratio	GPS	The ratio of time spent at the most frequently visited place, supposedly home. The identification of home follows these steps: (1) the most frequent values of coordinates in the time range of 2 a.m. and 5 a.m. are found; (2) these coordinates are assigned to “home” coordinates; (3) 10 m radius is attributed to the same place.
Distance to home	GPS	The average distance to home per day (km). The distance to the coordinates, which were assigned to home, is calculated using pointDistance function (<i>raster</i> library, RStudio).
Places of interest (POI)	GPS	The number of places of interest (POI) per day. POI is described as the place in which a patient spends not less than 30 min. The location is evaluated from coordinates. 100 m radius is attributed to the same place.
Screen time ratio	Power State	The ratio of smartphone screen on duration per day.

We conducted an exploratory data analysis to characterize distributions, ranges, and missing-data patterns of all passively generated variables. Summary statistics (N, mean, SD, minimum, maximum, and missing-data percentage) were computed for each sensor-derived feature (Supplement Table S1).

The EDA revealed substantial heterogeneity in mobility and activity patterns, with higher missingness in accelerometer-based metrics ($\approx 52\%$) and lower missingness in GPS-derived variables ($\approx 5\%$). Screen-state data showed moderate missingness ($\approx 36\%$). These

findings informed model selection and reinforced the need for individualized baselines rather than population-level thresholds.

2.4. Complications

Treatment complications were prospectively recorded throughout the study period by the study physicians during routine clinic visits and by reviewing medical records and contacting patients. Only complications that occurred after patient inclusion were analyzed to avoid retrospective bias. Because the number of events for individual complication types was small, complications were analyzed as a single aggregated outcome. This decision was made to ensure statistical feasibility; however, heterogeneity limits interpretability and clinical specificity. The present analysis did not include stratified modeling by complication subtype due to limited event counts. Larger datasets will enable subtype-specific analyses and the assessment of whether different complication categories exhibit distinct predictive behavioral patterns.

2.5. Symptoms

Symptom severity was evaluated using the European Organization for Research and Treatment of Cancer Core Quality of Life questionnaire (EORTC QLQ-C30) [41], completed by patients every two weeks through the LAIMA application. Each item is scored from 1 (“Not at all”) to 4 (“Very much”), and the Lithuanian translation is validated [37]. The following symptoms were analyzed: vomiting, nausea, diarrhea, fatigue, depression, appetite loss and insomnia. Worsening of symptoms was defined as the first occurrence of reporting a symptom as “quite a bit” or “very much” when it had not been reported at that level previously. Fatigue was defined using four EORTC QLQ-C30 items (Are you tired of a short walk after leaving home?; Are you forced to lie in bed or sit in an armchair during the day?; Did you feel weak?; and Did you feel tired?) a single positive answer indicated fatigue presence. Depression was assessed using the question “Did you feel depressed?”, diarrhea using “Have you had diarrhea?”, and vomiting using “Have you vomited?”.

To ensure consistency across assessments, only symptom reports occurring within the predefined two-week questionnaire cycle were included in analyses. Missing responses were handled according to EORTC scoring guidelines—symptoms were considered “absent” only if the corresponding item was explicitly answered as 1 (“Not at all”).

Patients continued completing the questionnaire until study completion or voluntary withdrawal (Figure 2).

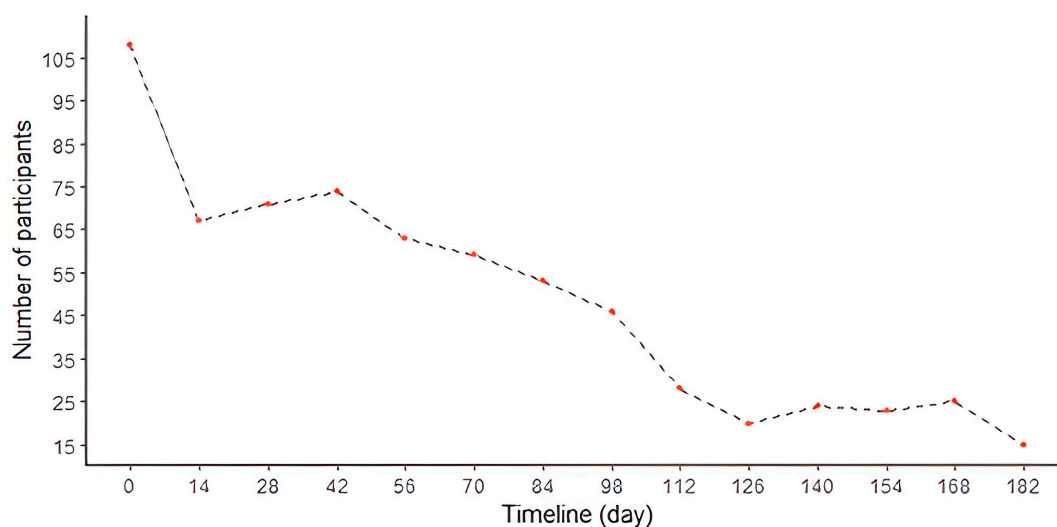


Figure 2. Number of patients who answered questionnaires during study.

2.6. Dataset Structure and Analytical Tasks

To improve transparency and clarify the structure of the dataset and analytical objectives, Figure 3 provides a schematic overview of the complete data-processing and modeling pipeline used in this study.

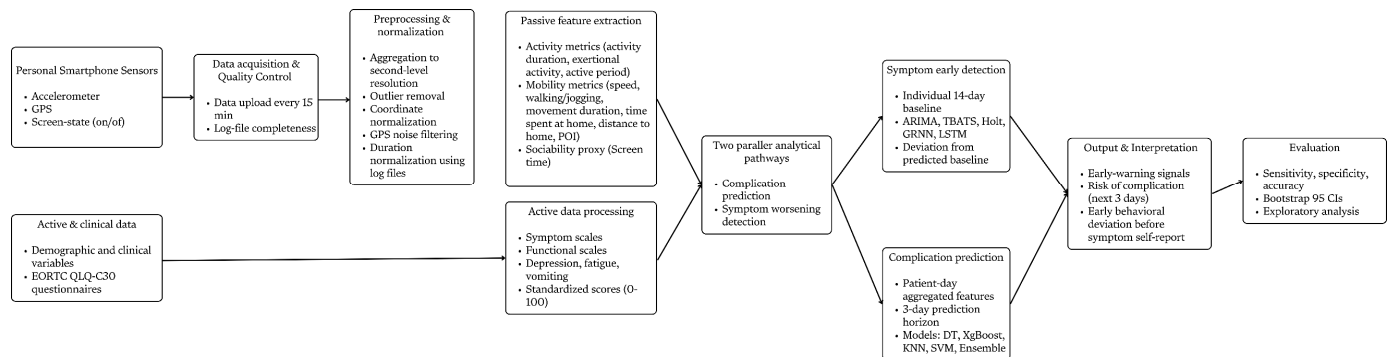


Figure 3. Dataset structure and analytical workflow of the proposed multi-sensor framework.

Passively collected smartphone data were acquired from personal devices using accelerometer, GPS, and screen-state sensors. Sensor data were transmitted approximately every 15 min (or buffered and uploaded when network connectivity became available) and were stored with timestamps, sensor identifiers, and patient IDs. Log files were additionally used for quality control to assess daily data completeness and identify potential data-flow interruptions.

Raw sensor streams underwent preprocessing and normalization, including aggregation to second-level resolution, noise and outlier filtering, GPS artifact removal, and normalization of duration-based variables using log-file completeness information. From these cleaned signals, a set of daily behavioral features was extracted, representing physical activity, mobility, and sociability proxies.

In parallel, actively collected clinical and questionnaire data—including demographic variables, clinical characteristics, and EORTC QLQ-C30 symptom assessments—were processed to derive standardized symptom and functional scores.

The resulting dataset supports two distinct but complementary analytical tasks, illustrated in Figure 3.

Short-term complication prediction, formulated as a supervised classification task. Patient-day-level aggregated behavioral and clinical features were used to predict whether a patient would experience a cancer-related complication within the subsequent three days. This task employed multiple machine learning classifiers (Decision Tree, XGBoost, K-Nearest Neighbors, Support Vector Machine) and an ensemble model.

Early symptom deviation detection, formulated as a patient-specific time-series forecasting task. For each patient, individualized 14-day behavioral baselines were modeled using time-series methods (ARIMA, TBATS, Holt, GRNN, LSTM). Deviations of observed values beyond the 95% prediction intervals were interpreted as early-warning signals preceding self-reported symptom worsening.

Model outputs from both analytical pathways were designed to generate interpretable early-warning signals, enabling assessment of short-term complication risk and behavioral deviation prior to clinical or questionnaire-based symptom recognition.

Importantly, these two analytical tasks address different clinical questions and are not directly comparable using a single performance metric. Classification focuses on identifying short-term risk, whereas forecasting focuses on detecting within-patient behavioral deviations.

2.7. Statistical Analysis

Distributions of clinical and demographical parameters between patients with or without complications and symptoms were compared using the χ^2 test, with a significance level of 0.05. To evaluate short-term prediction of complications (within 3 days), four machine learning classifiers were applied: Decision Tree, Extreme Gradient Boosting, K-Nearest Neighbors, and Support Vector Machine. An ensemble model was created to improve the models' accuracy. A 3-day prediction window was selected because exploratory analysis showed that behavioral deviations typically emerged 2–3 days before complication diagnosis, whereas longer windows diluted the signal. To provide more robust performance estimates and address concerns of statistical instability, 95% bootstrap confidence intervals were calculated for accuracy, sensitivity, and specificity. Model performance was assessed using accuracy, sensitivity, specificity, and confusion matrices. To detect symptom worsening earlier than patient self-report, individualized behavioral baselines of activity and sociability were modeled using time-series models: ARIMA, Holt–Winters, TBATS, LSTM, and GRNN. For each model, 95% prediction intervals were generated to characterize uncertainty in time-series forecasts.

The analysis was performed using RStudio (version 2022.12.0+353; R 4.2.2) and Jupyterlab (version 3.5.3; Python 3.10.9). Descriptive statistics are presented as frequencies (percentages).

3. Results

3.1. Clinical and Demographic Data of the Patients

The study cohort included 108 patients with cancer (60.2% females, mean age 56.1 ± 16.2). Most patients had college degree (61.1%), were married or in a relationship (72.2%), lived in urban area (71.3%), were employed (57.4%), and had an Android smartphone (92.6%). Most common cancer diagnoses were cervical (18.5%), prostate (17.6%), breast (12.9%), uterine (12.9%), and digestive tract (9.2%) cancer, followed by hematologic (5.6%), mouth (4.6%), lung (3.7%), and other types of cancer (13.9%). Less than half of patients had a history of systemic treatment (42.6%), while most were undergoing systemic therapy (67.6%) and radiotherapy (57.4%). Most patients (87%) had ECOG 0 and were fully active.

Prior to study enrollment, 78 patients had already experienced complications; during the study, 25.9% developed at least one new complication. The occurrence of complications differed across cancer type ($p = 0.019$), with breast, prostate, and uterine cancers showing fewer complications, whereas four out of five patients with mouth cancer experienced a complication.

All 108 patients completed self-reported symptom assessments, of whom 71 reported new or worsening symptoms. Clinical and demographic characteristics remained similar between patients with and without symptom worsening.

Symptom worsening was more prevalent among women ($p = 0.001$) and varied across cancer types ($p = 0.001$), but no associations were observed with other demographic or clinical parameters. Table 2 summarizes the distribution of demographic and clinical characteristics by complication status and symptom worsening.

The χ^2 test compares categorical distributions between groups; however, due to small subgroup sizes, the resulting p -values may be unstable and should be interpreted with caution.

Table 2. Patients demographic and clinical characteristics with and without complications, and with and without symptom worsening.

Clinical and demographic parameter	Characteristic	Complications		χ^2 p-value	Symptoms		χ^2 p-value
		Yes n = 28 (25.9%)	No n = 80 (74.1%)		Yes n = 71 (65.7%)	No n = 37 (34.3%)	
Age	18–25	2 (7.1)	2 (2.5)	4.891 0.179	2 (2.8)	2 (5.4)	3.295 0.348
	26–40	2 (7.1)	11 (13.7)		12 (16.9)	2 (5.4)	
	41–64	18 (64.3)	37 (46.3)		34 (47.9)	21 (56.8)	
	≥65	6 (21.5)	30 (37.5)		23 (32.4)	12 (32.4)	
Sex	Male	11 (39.3)	32 (40.0)	0.000	20 (28.2)	23 (62.2)	10.353
	Female	17 (60.7)	48 (60.0)	1.000	51 (71.8)	14 (37.8)	0.001
Education	With Academic degree	14 (50.0)	52 (65.0)	1.383	49 (69.0)	18 (48.6)	3.462
	Without Academic degree	14 (50.0)	28 (35.0)	0.239	22 (31.0)	19 (51.4)	0.062
Marital status	Single	3 (10.7)	7 (8.8)	0.532 0.911	5 (7.0)	5 (13.5)	3.146 0.369
	Married	19 (67.9)	59 (73.8)		50 (70.4)	28 (75.7)	
	Divorced	2 (7.1)	6 (7.5)		6 (8.5)	2 (5.4)	
	Widowed	4 (14.3)	8 (10.0)		10 (14.1)	2 (5.4)	
Living area	Urban	20 (71.4)	57 (71.3)	0.000	47 (66.2)	30 (81.1)	1.956
	Rural	8 (28.6)	23 (28.7)	1.000	24 (33.8)	7 (18.9)	0.161
Occupation and employment status	Employed	15 (53.6)	45 (56.3)	3.585 0.309	44 (62.0)	18 (48.6)	6.895 0.075
	Unemployed	1 (3.6)	5 (6.2)		4 (5.6)	1 (2.7)	
	Retired	7 (25.0)	25 (31.3)		20 (28.2)	11 (29.7)	
	Other	5 (17.8)	5 (6.2)		3 (4.2)	7 (18.9)	
Smartphone operating system	Android	26 (92.9)	74 (92.5)	0.375	65 (91.5)	34 (91.9)	2.223
	iOS	2 (7.1)	5 (6.3)	0.828	6 (8.5)	2 (5.4)	0.328
	Other	0 (0)	1 (1.2)		0 (0)	1 (2.7)	
Cancer type	Breast	2 (7.1)	12 (15.0)	19.684 0.019	12 (16.9)	3 (8.1)	26.525 0.001
	Cervix	6 (21.5)	14 (17.5)		17 (23.9)	3 (8.1)	
	Prostate	2 (7.1)	17 (21.3)		7 (9.9)	12 (32.4)	
	Digestive tract	6 (21.5)	5 (6.2)		6 (8.5)	4 (10.8)	
	Lungs	2 (7.1)	2 (2.5)		1 (1.4)	3 (8.1)	
	Uterus	2 (7.1)	12 (15.0)		14 (19.7)	0 (0)	
	Hematological	1 (3.6)	5 (6.2)		4 (5.6)	2 (5.4)	
	Mouth	4 (14.3)	1 (1.3)		2 (2.8)	3 (8.1)	
	Other	3 (10.7)	12 (15.0)		8 (11.3)	7 (19.0)	
	History of systemic treatment	Yes	14 (50.0)		32 (40.0)	0.488	
No		14 (50.0)	48 (60.0)	0.484	42 (59.2)	20 (54.1)	0.761
Current systemic treatment	Yes	23 (82.1)	50 (62.5)	2.811	45 (63.4)	28 (75.7)	1.164
	No	5 (17.9)	30 (37.5)	0.093	26 (36.6)	9 (24.3)	0.280
Current radiotherapy	Yes	15 (53.6)	47 (58.8)	0.064	45 (63.4)	17 (49.9)	2.352
	No	13 (46.4)	33 (41.2)	0.799	26 (36.6)	20 (54.1)	0.125
ECOG	0	25 (89.3)	69 (86.2)	3.631 0.162	61 (85.9)	34 (91.9)	1.076 0.583
	1	2 (7.1)	11 (13.8)		9 (12.7)	3 (8.1)	
	2	1 (3.6)	0 (0)		1 (1.4)	0 (0)	

3.2. Identification of Complications

Overall, 28 patients experienced complication during the study period. The complications were clinically diverse, including anemia (n = 4), severe pain (n = 2), infection (n = 8; cholangitis, esophagitis, gonarthrosis, pneumonia, inflammation of the uterine appendages, sepsis, periodontitis), inflammatory (anaphylactic shock, exacerbation of bronchial asthma), need for unexpected surgery (need for laparotomy and tumor excision), cardiovascular (embolism, heart failure), and other (ascites, dysphagia, edema, epilepsy, hyponatremia, scratching, metastasis, progress, urinary retention, thrombocytopenia). Because complication types were highly heterogeneous and subgroup sizes were small, complications were analyzed as a single combined endpoint. The machine learning models used passively generated behavioral features (activity duration ratio, exertional activity duration ratio, active period, movement duration ratio, time spent at “home” ratio, distance to “home” (km), POI and screen time ratio) together with demographic and clinical characteristics (age, ECOG score, current radiotherapy, systemic treatment status) to predict whether a patient would develop a complication within the next three days. Behavioral changes were quantified by comparing each patient’s short-term window (days 1–3 before the complication) with a longer preceding window (days 4–17). For patients without compli-

cations, the first month after enrollment was evaluated using analogous windows (1–14 vs. 15–29 days). The intervals were determined by analyzing the data and noting the tendency of patients' behavior changes three days prior to the complication, whereas patients without complications continue their usual behavior during the first month of the study. Due to the limited dataset, an 80/20 train–test split was used. Overfitting risk cannot be completely eliminated in small-event settings and is considered in the interpretation of the results. Below are the machine learning models trained:

- Decision Tree (DT): The DT model was developed with the threshold of 20 minimum number of observations in a node and set the maximum depth of the tree to 30, as altering them did not yield improved results.
- Extreme Gradient Boosting (XgBoost): The XgBoost model employed cross-validation with five folds and learning rate of 0.4. The maximum depth of tree was set to one.
- K-Nearest Neighbor (KNN): The KNN model was constructed using seven nearest neighbors.
- Support Vector Machine (SVM): The SVM model was created using a linear function and featured 46 support vectors.
- Ensemble: The Ensemble model was created by combining all the obtained models results and predicted complications when at least one of all the models predicted it.

Passively collected smoothed (due to outlier sensitivity) data were used to create the prediction: activity duration, strenuous activity duration, active period duration, average speed, average walking speed, movement duration, time spent “at home”, distance to “home”, number of places visited and duration of unlocked phone. Demographic and clinical characteristics were also included: age, functional status assessment (ECOG), radiotherapy and systemic treatment status.

Table 3 presents performance metrics. None of the individual models exceeded 67% sensitivity, while specificity ranged from 75% to 100%. Given the clinical importance of sensitivity in oncology, the ensemble model correctly identified eight of nine patients with complications (sensitivity = 0.89; 95% CI 0.52–0.99) and nine of twelve patients without complications (specificity = 0.75; 95% CI 0.47–0.91) (Figure 4). However, given the small number of complication events ($n = 28$), performance estimates are inherently unstable and sensitive to individual observations. Therefore, Figure 3 should be interpreted as an illustrative example of model behavior rather than as definitive evidence of generalizable performance. The wide confidence intervals further reflect this uncertainty and underscore the exploratory nature of the presented results. Overall accuracy was 0.81 (95% CI 0.60–0.92). The ensemble approach substantially improved sensitivity compared with individual classifiers, which is clinically important for identifying patients at imminent risk.

Table 3. Accuracy metrics of complication prediction.

Metric	Accuracy	Specificity	Sensitivity
DT	76%	83%	67%
XgBoost	71%	100%	33%
KNN	62%	92%	22%
SVM	66%	92%	33%
Ensemble	81%	75%	89%

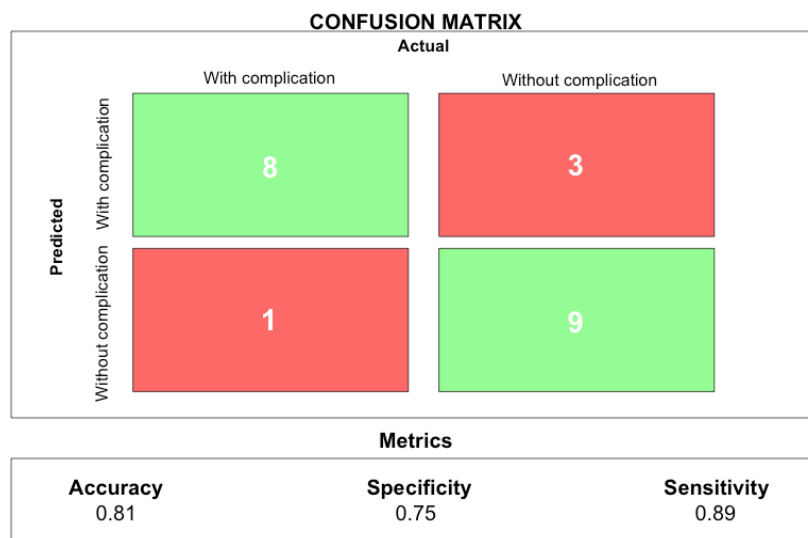


Figure 4. Confusion matrix of ensemble model predicting complications within three days.

3.3. Identification of New or Worsening Symptoms

Three symptoms—depression, fatigue, and vomiting—were found to be associated with measurable changes (increase or decrease) in activity and sociality derived from passively collected smartphone sensor data in the days preceding symptom worsening. We compared median values of behavioral indicators during the two-week window prior to symptom worsening with those from the preceding two-week baseline period. Behavioral characteristics that changed in more than 30% of affected patients were selected for symptoms profiling (Table 4). We found that 58.53% of patients who reported fatigue and 62.50% of patients who reported vomiting had decreased screen time. A shorter distance from home was observed in 73.91% of patients who reported depressive symptoms. These findings indicate that passively collected behavioral deviations frequently precede subjective symptom reporting, supporting the potential of digital biomarkers for early symptom detection.

To evaluate whether passive data could predict symptom worsening, we modeled each patient’s individualized behavior baseline using several forecasting algorithms (ARIMA, TBATS, Holt, GRNN, LSTM). The baseline period consisted of the 14 days preceding symptom onset. A 14-day baseline was chosen to align with the EORTC QLQ-C30 two-week assessment cycle and prior digital phenotyping studies using 14-day behavioral baselines. For each variable, the model with the lowest test Mean Absolute Error (MAE) was selected (Table 5). The best-performing models varied by behavioral variable: ARIMA and TBATS were optimal for three variables each, LSTM for two variables, and GRNN and Holt for one variable each.

Table 4. Proportion of patients showing decreased or increased activity and sociability indicators prior to symptom worsening (depression, fatigue, vomiting).

Variable	Number of Patients with Decreased (Increased) Activity and Sociability (%)	Decreased or Increased
Depression		
Screen time ratio	7 out of 23 (30.43%)	Increased
Movement duration ratio	12 out of 23 (52.17%)	Decreased
Distance from home	17 out of 23 (73.91%)	Decreased

Table 4. *Cont.*

Variable	Number of Patients with Decreased (Increased) Activity and Sociability (%)	Decreased or Increased
Fatigue		
Screen time ratio	24 out of 41 (58.53%)	Decreased
Time spent at home ratio	20 out of 41 (48.78%)	Increased
Distance from home	18 out of 41 (43.90%)	Decreased
Average speed of movement	18 out of 41 (43.90%)	Decreased
Vomiting		
Activity frequency	3 out of 8 (37.50%)	Decreased
Screen time ratio	5 out of 8 (62.50%)	Decreased
Time spent at home ratio	3 out of 8 (37.50%)	Increased

Table 5. Most suitable models for variables.

Variable	Model	MAE (95% CI)
Depression		
Screen time ratio	Tbats	0.32 (0.01–2.05)
Movement duration ratio	LSTM	0.21 (0.01–0.94)
Distance from home	ARIMA	9.30 (0.15–11.85)
Fatigue		
Screen time ratio	Tbats	0.47 (0.02–1.71)
Time spent at home ratio	LSTM	0.05 (0.01–0.10)
Distance from home	GRNN	15.41(4.43–29.67)
Average speed of movement	Tbats	0.03 (0.01–0.16)
Vomiting		
Activity frequency	Holt	0.03 (0.01–0.16)
Screen time ratio	ARIMA	0.32 (0.02–1.03)
Time spent at home ratio	ARIMA	0.06 (0.01–0.11)

Next, we evaluated whether the actual values of the averaged smartphone sensor data deviated from the predicted baseline. The baseline reflected each patient’s typical behavior during two weeks prior to symptom onset and was forecasted using the model with the lowest MAE (Table 5). Deviation was flagged when the actual value fell outside the 95% confidence interval. This approach focuses on detecting within-patient behavioral deviations rather than achieving precise point forecasts. Therefore, the results should be interpreted as indicative of atypical behavioral patterns relative to an individual baseline, even when confidence intervals are wide. The wide confidence intervals observed for several MAE estimates reflect the small sample sizes and inter-patient variability, indicating substantial uncertainty in model performance. An example is shown in Figure 5. A decreasing distance from home (panel a) indicated a deviation two days before the patient self-reported depression. A reduction in screen time ratio (panel b) indicated deviation six days before self-report.

Overall, early detection of self-reported depression was achieved in 38.47% of patients when using screen time as the predictor, with symptoms detected 9 ± 4.47 days earlier compared with questionnaire-based reporting. Fatigue was identified in 26.83% of patients an average of 9 ± 2.91 days before self-report using distance from home. Vomiting was detected 9 ± 4.04 days earlier in 33.33% of the patients using screen time ratio (Table 6).

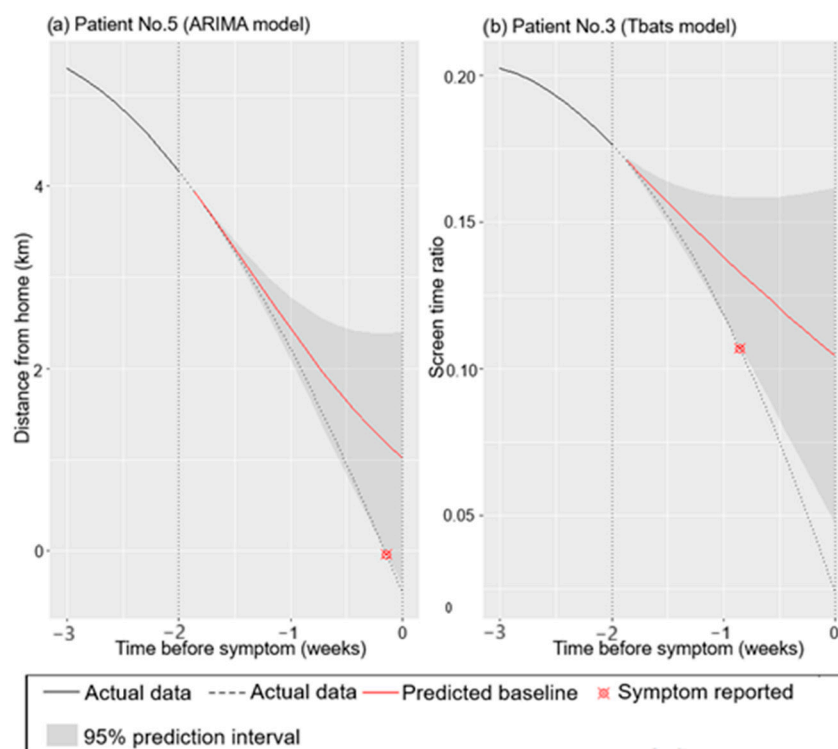


Figure 5. Identification of depression by (a) distance from home forecast; (b) screen time ratio forecast.

Table 6. Early detection of symptoms using passively generated smartphone sensor data.

Variable	Days Before Determining (Mean ± SD)	The Number of Patients with Symptoms Detected Earlier (%)
Depression		
Screen time ratio	9 ± 4.47	10 out of 23 (38.47%)
Distance from home	8 ± 6.11	7 out of 23 (26.93%)
Fatigue		
Screen time ratio	7 ± 4.92	12 out of 41 (29.28%)
Distance from home	9 ± 2.91	11 out of 41 (26.83%)
Average speed of movement	7 ± 4.70	12 out of 41 (29.28%)
Vomiting		
Screen time ratio	9 ± 4.04	3 out of 8 (33.33%)

Early detection in this context refers to the identification of behavioral deviations preceding patient self-reported symptom worsening and does not imply clinical diagnosis, causal inference, or outcome prediction.

4. Discussion

In this exploratory study, we evaluate the feasibility of using passively generated smartphone sensor data to identify behavioral deviations that precede treatment- or cancer-related complications and symptom worsening. To the best of our knowledge, this study is among the first to integrate accelerometer, GPS, and screen-state data during active cancer treatment within a unified exploratory analytical framework.

In this study, AI-based models were used to explore whether changes in accelerometer, GPS, and screen-state data streams could precede clinically diagnosed or self-reported complications by several days. These findings indicate that impending complications may manifest as subtle behavioral deviations detectable through passive sensors. We also demonstrated that passive smartphone data can identify worsening depression, fatigue,

and vomiting, highlighting its potential for remote monitoring of patient-reported outcomes (PROs). Early recognition of symptom deterioration is clinically relevant and may support timely interventions, particularly in patients with advanced or incurable cancer [42]. Our results are aligned with previous work showing that smartphone-based passive sensing can detect mental health symptoms in college students [43] and individuals with depression [44], but our study extends this approach to oncology patients during active treatment.

However, earlier detection refers to behavioral deviation before self-reported symptoms—not clinically confirmed onset. Self-report remains the clinical ground truth for subjective symptoms such as fatigue, depression, and nausea; thus, our findings indicate a digital early-warning signal rather than definitive diagnostic detection.

Treatment-related complications are common among patients receiving chemotherapy and radiotherapy. Many patients present to the emergency department (ED) for evaluation of complications, contributing to hospital admissions and substantial healthcare costs. Prior studies reported that patients with breast, prostate, and lung cancer frequently seek ED care, with neutropenia, sepsis, and anemia being the most common causes [9,45]. Given this burden, early identification of patients at risk of complications may reduce avoidable ED visits, hospitalizations, and morbidity. Existing eHealth tools rely mainly on symptom surveys or behavioral interventions [42,46–48], whereas our findings show that passive smartphone sensing may complement these approaches by enabling continuous monitoring without patient burden.

Evidence on passively generated smartphone accelerometer and GPS data in oncology is limited. A prior study of 62 patients after cancer surgery showed that smartphone accelerometer data differentiated activity patterns among patients with and without postoperative event [40]. Another study involving GPS monitoring after breast cancer surgery found that patients after mastectomy spent more time at home and traveled shorter distances [49]. Our study expands on this literature by integrating multiple passive sensors and demonstrating feasibility for monitoring patients undergoing active treatment, not only postoperative recovery.

Previous work has shown that integrating accelerometer and GPS signals can detect mental health symptoms such as depression, anxiety, and loneliness [43,49], but these studies were conducted in non-oncology population. Thus, our study addresses an important gap by evaluating passive sensing specifically in cancer cohort.

The selection of ML and time-series algorithms must balance performance, interpretability, and data requirements.

SVM performs well in high-dimensional settings but is sensitive to noise; KNN is intuitive but computationally intensive and not robust to outliers; Decision Tree may overfit on small datasets.

ARIMA and Holt methods are easy to interpret but assume stationarity; GRNN and LSTM can model nonlinear patterns but require large datasets and greater computational resources. Because behavioral deviations preceding complications are subtle, noisy, and heterogeneous, the passive-sensing features were largely non-linearly separable. This explains the low sensitivity observed in linear and distance-based classifiers and the improved performance of the ensemble model.

Importantly, the observed high sensitivity of the ensemble model must be interpreted in the context of the limited complication sample size. Although confidence intervals were estimated using bootstrapping, the small number of events introduces statistical instability, which may inflate apparent performance. Consequently, the current results demonstrate feasibility rather than robust predictive accuracy and require confirmation in larger, independent cohorts.

Early detection of symptom worsening is promising, but clinical use requires clear alert-handling rules. In practice, deviations beyond the 95% prediction-interval bounds could function as automated alert thresholds. Clinically actionable symptoms—such as vomiting, severe fatigue, or depressive worsening—would justify patient contact, triage, or treatment adjustments. Integration would occur through clinician dashboards showing deviations from individualized baselines. Prospective trials are needed to validate thresholds, quantify false-alert rates, and assess clinical utility before implementation.

Although point estimates of MAE were relatively low, the wide 95% prediction intervals indicate substantial uncertainty in model performance estimates. This likely reflects the limited sample size, inter-individual heterogeneity, and irregularity of symptom trajectories. Therefore, the reported results should be interpreted as exploratory and hypothesis-generating rather than confirmatory. The primary contribution of this analysis lies in demonstrating that deviations from individualized behavioral baselines can precede symptom self-report, rather than in providing stable or generalizable error bounds.

Several limitations should be acknowledged. First, due to the small number and heterogeneity of complications, we were unable to evaluate feasibility of detecting specific complication types. Second, some events or symptom worsening may reflect cancer progression rather than treatment-related complications, although the short follow-up reduces this likelihood. Third, variability in smartphone usage habits and baseline activity patterns may influence sensor-derived metrics; however we analyzed within-person behavioral changes rather than absolute values to reduce bias. In addition, several external confounders may influence behavioral variables independently of symptoms, including weather conditions, transportation availability, work schedules, or social events that affect mobility patterns. Fourth, the short follow-up period limits conclusions about long-term survivorship monitoring. The single-center Lithuanian cohort and predominance of Android devices further limit generalizability. Fifth, symptom-specific analyses—particularly for vomiting ($n = 8$)—were limited by small sample size, and these findings should be interpreted as exploratory rather than definitive. Finally, sensor noise, missing data, and algorithmic bias may affect model stability, and these issues are discussed in this and the Methods sections.

Studies with larger and more diverse cohorts are needed to evaluate clinical utility, optimize models, and determine feasibility for real-world deployment.

5. Conclusions

We evaluated the feasibility of using passively generated personal smartphone sensor data to explore behavioral changes preceding cancer-related complications and symptoms worsening during active treatment. By integrating accelerometer, GPS, and screen-state data into a unified analytical framework, this study demonstrates how multi-sensor passive data can be transformed into individualized behavioral baselines for exploratory monitoring. Using complementary analytical tasks—including short-term complication classification and patient-specific time-series deviation detection—we observed that deviations from personalized behavioral baselines could precede self-reported symptom worsening and clinically recorded complications by several days in a subset of patients. However, wide uncertainty intervals, heterogeneous complication types, and limited event counts indicate that these findings should be interpreted as exploratory and hypothesis-generating rather than confirmatory. The primary contribution of this work lies in methodological demonstration and feasibility assessment rather than in establishing stable or generalizable predictive performance. Larger studies are needed to validate these findings, evaluate generalizability across diverse patient populations, smartphone platforms, and cancer types, and assess prospective clinical utility within real-world oncology workflows.

Supplementary Materials: The following supporting information can be downloaded at: <https://www.mdpi.com/article/10.3390/app16010249/s1>, Table S1: Summary of passive-sensor features including distribution statistics and percentage of missing data.

Author Contributions: Conceptualization, T.K. and A.B.; methodology, G.D., G.K. and P.S.; validation, E.K., D.V., A.I., L.J., R.K., T.K., E.J. and A.B.; formal analysis, G.K., G.D., P.S. and R.K.; investigation, E.K., D.V., A.I., L.J. and A.B.; data curation, G.D., G.K., P.S. and E.K.; writing—original draft preparation, G.D., G.K., P.S., A.B., I.B., E.K., D.V., A.I., L.J., R.B., R.K., T.K. and E.J.; writing—review and editing, G.D., G.K., I.B., E.K., D.V., A.I., L.J., R.B., R.K., T.K. and E.J.; visualization, G.D. and G.K.; supervision, E.J., A.B., R.K. and T.K.; project administration, I.B.; funding acquisition, R.K. and T.K. All authors have read and agreed to the published version of the manuscript.

Funding: The research was co-funded by the European Union under Horizon Europe program grant agreement No. 101059903, by the European Union funds for the period 2021–2027, and by the state budget of the Republic of Lithuania financial agreement Nr. 10-042-P-0001.

Institutional Review Board Statement: The study was conducted in accordance with the Declaration of Helsinki and approved by the Kaunas Regional Biomedical Research Ethics Committee (protocol code BE-2-31, approval date 14 April 2022).

Informed Consent Statement: Informed consent was obtained from all subjects involved in the study.

Data Availability Statement: The raw data supporting the conclusions of this article will be made available by the authors, without undue reservation.

Conflicts of Interest: Author Romas Bunevičius was employed by the company ProIT. The remaining authors declare that the research was conducted in the absence of any commercial or financial relationships that could be construed as a potential conflict of interest.

References

1. Ferlay, J.; Colombet, M.; Soerjomataram, I.; Parkin, D.M.; Piñeros, M.; Znaor, A.; Bray, F. Cancer statistics for the year 2020: An overview. *Int. J. Cancer* **2021**, *149*, 778–789. [[CrossRef](#)]
2. Henry, D.H.; Viswanathan, H.N.; Elkin, E.P.; Traina, S.; Wade, S.; Cella, D. Symptoms and treatment burden associated with cancer treatment: Results from a cross-sectional national survey in the U.S. *Support. Care Cancer* **2008**, *16*, 791–801. [[CrossRef](#)]
3. Epstein, J.B.; Thariat, J.; Bensadoun, R.; Barasch, a.; Murphu, B.A.; Kolnick, L.; Popplewell, L.; Maghami, E. Oral complications of cancer and cancer therapy. *CA A Cancer J. Clin.* **2012**, *62*, 400–422. [[CrossRef](#)]
4. Yeh, E.; Bickford, C. Cardiovascular Complications of Cancer Therapy. *J. Am. Coll. Cardiol.* **2009**, *53*, 2231–2247. [[CrossRef](#)]
5. Graus, F.; Rogers, L.; Posner, J. Cerebrovascular Complications in Patients with Cancer. *Medicine* **1985**, *64*, 16–35. [[CrossRef](#)]
6. Altun, İ.; Sonkaya, A. The Most Common Side Effects Experienced by Patients Were Receiving First Cycle of Chemotherapy. *Iran. J. Public. Health* **2018**, *47*, 1218–1219.
7. Dennert, G.; Horneber, M. Selenium for alleviating the side effects of chemotherapy, radiotherapy and surgery in cancer patients. *Cochrane Database Syst. Rev.* **2006**, *3*, Art. No., CD005037. [[CrossRef](#)]
8. Löbrich, M.; Kiefer, J. Assessing the likelihood of severe side effects in radiotherapy. *Int. J. Cancer* **2006**, *118*, 2652–2656. [[CrossRef](#)]
9. Jairam, V.; Lee, V.; Park, H.S.; Thomas, C.R.; Melnick, E.R.; Gross, C.P.; Presley, C.J.; Adelson, K.B.; Yu, J.B. Treatment-Related Complications of Systemic Therapy and Radiotherapy. *JAMA Oncol.* **2019**, *5*, 1028–1035. [[CrossRef](#)] [[PubMed](#)] [[PubMed Central](#)]
10. McGregor, B.A.; Vidal, G.A.; Shah, S.A.; Mitchell, J.D.; Hendifar, A.E. Remote Oncology Care: Review of Current Technology and Future Directions. *Cureus* **2020**, *12*, e10156. [[CrossRef](#)] [[PubMed](#)] [[PubMed Central](#)]
11. Wells, M. Key components of successful digital remote monitoring in oncology. *Nat. Med.* **2022**, *28*, 1128–1129. [[CrossRef](#)]
12. Fouad, H.; Hassanein, A.S.M.; Soliman, A.M.; Al-Feel, H. Analyzing patient health information based on IoT sensor with AI for improving patient assistance in the future direction. *Measurement* **2020**, *159*, 107757. [[CrossRef](#)]
13. Spanò, E.; Di Pascoli, S.; Iannaccone, G. Low-Power Wearable ECG Monitoring System for Multiple-Patient Remote Monitoring. *IEEE Sens. J.* **2016**, *16*, 5452–5462. [[CrossRef](#)]
14. Morales-Botello, M.L.; Gachet, D.; de Buenaga, M.; Aparicio, F.; Busto, M.J.; Ascanio, J.R. Chronic patient remote monitoring through the application of big data and internet of things. *Health Inform. J.* **2021**, *27*, 1–18. [[CrossRef](#)]
15. Mohammed, J.; Lung, C.H.; Oceanu, A.; Thakral, A.; Jones, C.; Adler, A. Internet of Things: Remote Patient Monitoring Using Web Services and Cloud Computing. In Proceedings of the 2014 IEEE International Conference on Internet of Things (iThings),

- and IEEE Green Computing and Communications (GreenCom) and IEEE Cyber, Physical and Social Computing (CPSCom), Taipei, Taiwan, 1–3 September 2014; pp. 256–263. [\[CrossRef\]](#)
16. Kofoed, S.; Breen, S.; Gough, K.; Aranda, S. Benefits of remote real-time side-effect monitoring systems for patients receiving cancer treatment. *Oncol. Rev.* **2012**, *6*, e7. [\[CrossRef\]](#)
 17. Majumder, S.; Deen, M.J. Smartphone Sensors for Health Monitoring and Diagnosis. *Sensors* **2019**, *19*, 2164. [\[CrossRef\]](#)
 18. Papachristou, N.; Puschmann, D.; Barnaghi, P.; Cooper, B.; Hu, X.; Maguire, R.; Apostolidis, K.; Conley, Y.P.; Hammer, M.; Katsaragakis, S.; et al. Learning from data to predict future symptoms of oncology patients. *PLoS ONE* **2018**, *13*, e0208808. [\[CrossRef\]](#)
 19. Kooten, R.T.; Bahadoer, R.R.; Buurkes de Vries, B.; Wouters, M.W.J.M.; Tollenaar, R.A.E.M.; Hartgrink, H.H.; Putter, H.; Dikken, J.L. Conventional Regression Analysis and Machine Learning in Prediction of Anastomotic Leakage and Pulmonary Complications after Esophagogastric Cancer Surgery. *J. Surg. Oncol.* **2022**, *126*, 490–501. [\[CrossRef\]](#)
 20. Massaad, E.; Bridge, C.P.; Kiapour, A.; Fourman, M.S.; Duvall, J.B.; Connolly, I.D.; Hadzipasic, M.; Shankar, G.M.; Andriole, K.P.; Rosenthal, M.; et al. Evaluating frailty, mortality, and complications associated with metastatic spine tumor surgery using machine learning–derived body composition analysis. *J. Neurosurg. Spine* **2022**, *37*, 263–273. [\[CrossRef\]](#)
 21. Yeh, C.H.; Chiang, Y.C.; Chien, L.C.; Lin, L.; Yang, C.-P.; Chuang, H.-L. Symptom clustering in older Taiwanese children with cancer. *Oncol. Nurs. Forum* **2008**, *35*, 273–281. [\[CrossRef\]](#)
 22. Baggott, C.; Cooper, B.A.; Marina, N.; Matthay, K.K.; Miaskowski, C. Symptom cluster analyses based on symptom occurrence and severity ratings among pediatric oncology patients during myelosuppressive chemotherapy. *Cancer Nurs.* **2012**, *35*, 19–28. [\[CrossRef\]](#)
 23. Hockenberry, M.J.; Hooke, M.C.; McCarthy, K.; Gregurich, M.A. Sickness Behavior Clustering in Children with Cancer. *J. Pediatr. Oncol. Nurs.* **2011**, *28*, 263–272. [\[CrossRef\]](#)
 24. Hockenberry, M.J.; Hooke, M.C.; Gregurich, M.; McCarthy, K.S.; Sambuco, G.; Krull, K.R. Symptom clusters in children and adolescents receiving cisplatin, doxorubicin, or ifosfamide. *Oncol. Nurs. Forum* **2010**, *37*, E16–E27. [\[CrossRef\]](#)
 25. Neijenhuijs, K.I.; Peeters, C.F.W.; van Weert, H.; Cuijpers, P.; Leeuw, I.C.-de. Symptom clusters among cancer survivors: What can machine learning techniques tell us? *BMC Med. Res. Methodol.* **2021**, *21*, 166. [\[CrossRef\]](#)
 26. Absolom, K.; Warrington, L.; Hudson, E.; Hewison, J.; Morris, C.; Holch, P.; Carter, R.; Gibson, A.; Holmes, M.; Clayton, B.; et al. Phase III randomized controlled trial of eRAPID: eHealth intervention during chemotherapy. *J. Clin. Oncol.* **2021**, *39*, 734–747. [\[CrossRef\]](#)
 27. Bufano, P.; Laurino, M.; Said, S.; Tognetti, A.; Menicucci, D. Digital phenotyping for monitoring mental disorders: Systematic review. *J. Med. Internet Res.* **2023**, *25*, e46778. [\[CrossRef\]](#)
 28. Ingwersen, E.W.; Stam, W.T.; Meijs, B.J.V.; Roor, J.; Besselink, M.G.; Koerkamp, B.G.; de Hingh, I.H.J.T.; van Santvoort, H.C.; Stommel, M.W.J.; Daams, F. Machine learning versus logistic regression for the prediction of complications after pancreatoduodenectomy. *Surgery* **2023**, *174*, 435–440. [\[CrossRef\]](#)
 29. Arvind, V.; Kim, J.S.; Oermann, E.K.; Kaji, D.; Cho., S.K. Predicting Surgical Complications in Adult Patients Undergoing Anterior Cervical Discectomy and Fusion Using Machine Learning. *Neurospine* **2018**, *15*, 329–337. [\[CrossRef\]](#)
 30. Shima, M.; Ezz, M.; Hashem, S.; Elaken, W.; Salama, R.; ElMakhzangy, H.; ElHefnawi, M. Performance of machine learning approaches on prediction of esophageal varices for Egyptian chronic hepatitis C patients. *Inform. Med. Unlocked* **2019**, *17*, 100267. [\[CrossRef\]](#)
 31. Nudel, J.; Bishara, A.M.; de Geus, S.W.L.; Patil, P.; Srinivasan, J.; Hess, D.T.; Woodson, J. Development and validation of machine learning models to predict gastrointestinal leak and venous thromboembolism after weight loss surgery: An analysis of the MBSAQIP database. *Surg. Endosc.* **2021**, *35*, 182–191. [\[CrossRef\]](#)
 32. Zhou, X.; Wang, H.; Xu, C.; Peng, L.; Xu, F.; Lian, L.; Deng, G.; Ji, S.; Hu, M.; Zhu, H.; et al. Application of kNN and SVM to predict the prognosis of advanced schistosomiasis. *Parasitol. Res.* **2022**, *121*, 2457–2460. [\[CrossRef\]](#)
 33. Watson, L.; Qi, S.; DeLure, A.; Link, C.; Chmielewski, L.; Hildebrand, A.; Rawson, K.; Ruether, D. Using Autoregressive Integrated Moving Average (ARIMA) Modelling to Forecast Symptom Complexity in an Ambulatory Oncology Clinic: Harnessing Predictive Analytics and Patient-Reported Outcomes. *Int. J. Environ. Res. Public Health* **2021**, *18*, 8365. [\[CrossRef\]](#)
 34. Medina, D.C.; Findley, S.E.; Guindo, B.; Doumbia, S. Forecasting non-stationary diarrhea, acute respiratory infection, and malaria time-series in Niono, Mali. *PLoS ONE* **2007**, *2*, e1181. [\[CrossRef\]](#)
 35. Saturi, S.; Sravani, M.; Hruthika, S.C.; Sambaraju, M.; Prudvendra, R.; Kiran, S. Development of Prediction and Forecasting Model for Dengue Disease Based on the Environmental Conditions Using LSTM. In *Data Engineering and Intelligent Computing; Lecture Notes in Networks and Systems*; Bhateja, V., Khin Wee, L., Lin, J.C.W., Satapathy, S.C., Rajesh, T.M., Eds.; Springer: Singapore, 2022; Volume 446. [\[CrossRef\]](#)
 36. Sharma, N.; Om, H. Usage of Probabilistic and General Regression Neural Network for Early Detection and Prevention of Oral Cancer. *Sci. World J.* **2015**, *2015*, 234191. [\[CrossRef\]](#)

37. Bunevičius, A.; Tamašauskas, Š.; Tamašauskas, A.; Deltuva, V. Evaluation of health-related quality of life in Lithuanian brain tumor patients using the EORTC brain cancer module. *Medicina* **2012**, *48*, 588–594. [[CrossRef](#)]
38. Regulation (EU) 2016/679 of the European Parliament and of the Council of 27 April 2016 on the protection of natural persons with regard to the processing of personal data and on the free movement of such data, and repealing Directive 95/46/EC (General Data Protection Regulation). *Off. J. Eur. Union* **2016**, *4*, 1–88.
39. Robert, J.; Hijmans van Etten, J. The Distance for Longitude/Latitude Data Uses Geographic Lib by C.F.F. Karney. Available online: <https://rdrr.io/cran/raster/man/pointDistance.html> (accessed on 3 September 2023).
40. Panda, N.; Solsky, I.; Huang, E.J.; Lipsitz, S.; Pradarelli, J.C.; Delisle, M.; Cusack, J.C.; Gadd, M.A.; Lubitz, C.C.; Mullen, J.T.; et al. Using Smartphones to Capture Novel Recovery Metrics After Cancer Surgery. *JAMA Surg.* **2020**, *155*, 123–129. [[CrossRef](#)]
41. Aaronson, N.K.; Ahmedzai, S.; Bergamn, B.; Bullinger, M.; Cull, A.; Duez, N.J.; Filiberti, A.; Flechtner, H.; Fleishman, S.B.; de Haes, J.C.J.M. The European Organization for Research and Treatment of Cancer QLQ-C30: A quality-of-life instrument for use in international clinical trials in oncology. *J. Natl. Cancer Inst.* **1993**, *85*, 365–376. [[CrossRef](#)]
42. Buneviciene, I.; Mekary, R.A.; Smith, T.R.; Onnela, J.-P.; Bunevicius, A. Can mHealth interventions improve quality of life of cancer patients? A systematic review and meta-analysis. *Crit. Rev. Oncol. Hematol.* **2021**, *157*, 103123. [[CrossRef](#)]
43. Melcher, J.; Hays, R.; Torous, J. Digital phenotyping for mental health of college students: A clinical review. *BMJ Ment. Health* **2020**, *23*, 161–166. [[CrossRef](#)]
44. De Angel, V.; Lewis, S.; White, K.; Oetzmann, C.; Leightley, D.; Oprea, E.; Lavelle, G.; Matcham, F.; Pace, A.; Mohr, D.C.; et al. Digital health tools for the passive monitoring of depression: A systematic review of methods. *npj Digit. Med.* **2022**, *5*, 3. [[CrossRef](#)]
45. Rivera, D.R.; Gallicchio, L.; Brown, J.; Liu, B.; Kyriacou, D.N.; Shelburne, N. Trends in Adult Cancer-Related Emergency Department Utilization: An Analysis of Data from the Nationwide Emergency Department Sample. *JAMA Oncol.* **2017**, *3*, e172450. [[CrossRef](#)]
46. Vercell, V.; Gasteiger, N.; Yorke, J.; Dowding, D. Patient-facing cancer mobile apps that enable patient reported outcome data to be collected: A systematic review of content, functionality, quality, and ability to integrate with electronic health records. *Int. J. Med. Inform.* **2023**, *170*, 104931. [[CrossRef](#)]
47. Charbonneau, D.H.; Hightower, S.; Katz, A.; Zhang, K.; Abrams, J.; Senfit, N.; Beebe-Dimmer, J.L.; Heath, E.; Eaton, T.; Thompson, H.S. Smartphone apps for cancer: A content analysis of the digital health marketplace. *Digit. Health* **2020**, *Volume 6*. [[CrossRef](#)]
48. Wright, A.A.; Raman, N.; Staples, P.; Schonholz, S.; Cronin, A.; Carlson, K.; Keating, N.L.; Onnela, J.-P. The HOPE Pilot Study: Harnessing Patient-Reported Outcomes and Biometric Data to Enhance Cancer Care. *JCO Clin. Cancer Inform.* **2018**, *2*, 1–12. [[CrossRef](#)]
49. Panda, N.; Solsky, I.; Hawrusik, B.; Liu, G.; Reeder, H.; Lipsitz, S.; Desai, E.V.; Lowery, K.W.; Miller, K.; Gadd, M.A.; et al. Smartphone Global Positioning System (GPS) Data Enhances Recovery Assessment After Breast Cancer Surgery. *Ann. Surg. Oncol.* **2021**, *28*, 985–994. [[CrossRef](#)]

Disclaimer/Publisher’s Note: The statements, opinions and data contained in all publications are solely those of the individual author(s) and contributor(s) and not of MDPI and/or the editor(s). MDPI and/or the editor(s) disclaim responsibility for any injury to people or property resulting from any ideas, methods, instructions or products referred to in the content.